EXAFS and XANES study of GaAs on Ga and As K edges

1993 J. Phys.: Condens. Matter 5 1643

(http://iopscience.iop.org/0953-8984/5/11/005)

J. Phys.: Condens. Matter 5 (1993) 1643–1654. Printed in the UK

EXAFS and XANES study of GaAs on Ga and As K edges

G Dalba†, D Diop†, P Fornasini†, A Kuzmin‡ and F Rocca§

† Dipartimento di Fisica, Università di Trento, I-38050 Povo (Trento), Italy
‡ Institute of Solid State Physics, University of Latvia, LV-1063 Riga, Latvia
§ Centro di Fisica degli Stati Aggregati ed Impianto Ionico del Consiglio Nazionale delle Ricerche e Istituto Trentino di Cultura, I-38050 Povo (Trento), Italy

Received 3 June 1992, in final form 21 December 1992

Abstract. The extended x-ray absorption fine structure (EXAFS) at the K edges of Ga and As has been calculated in the multiple-scattering approach using the fast spherical approximation. It is shown that, for both edges, multiple-scattering contributions are negligible for wavevector values greater than $3\,\text{Å}^{-1}$, and the single-scattering analysis can be used without significant loss of accuracy in that region. The calculated spectra are in good agreement with measurements at 77 K. The x-ray absorption near-edge structure (XANES) at both edges have been calculated by the continued-fraction expansion method. The origin of the main XANES features and the differences between Ga and As edges have been interpreted. The first main peak is attributed to the bound-to-bound $1s \rightarrow 4p$ transition. The second feature is a scattering resonance within the second coordination shell: its position is defined by the different phase shifts of the photoelectron wave under scattering from the Ga or As atoms.

1. Introduction

Gallium arsenide is a very useful material, whose applications for microelectronic devices and solid state lasers are well known. Its great importance for fundamental and applied physics has led to a large number of works on this compound, particularly in recent years [1]. To our knowledge, only two papers report a study of pure GaAs crystals by x-ray absorption spectroscopy [2, 3]. The first paper [2] was devoted to a general investigation of the influence of many-body effects on the extended x-ray absorption fine structure (EXAFS) of several different compounds, including GaAs. Both gallium and arsenic K edges were reported; the relative Debye–Waller (DW) factors for spectra measured at 80 and 300 K were obtained by the ratio method [4, 5], and their absolute values were evaluated using the Einstein and Debye vibrational models. This procedure allowed workers to get information on inelastic contributions, in particular the k dependence of the photoelectron mean-free paths. In the second paper [3] an attempt was made to evaluate the EXAFS at the Ga K edge by three different theoretical approaches, including multiple-scattering (MS) corrections. The agreement with the experimental data of [2] was only qualitative: the main features were reproduced, but their amplitudes and positions were rather different, especially at energies lower than 300 eV. Moreover, the DW factors of the outer shells were greatly overestimated.

Careful studies of EXAFS in compounds with well known structure and physical properties are important to gain a deeper understanding of the basic mechanism of

0953-8984/93/111643+12$07.50

EXAFS. In particular, large efforts are being made by various authors to obtain reliable *ab initio* calculations of EXAFS [6]. Great attention is also dedicated to the possibility of obtaining from EXAFS original information on the vibrational properties of crystals, exploiting the peculiar sensitivity of EXAFS to phonon polarization [6]. Moreover, an estimate of the MS contributions to EXAFS is necessary before attempting a study of the temperature dependence of the EXAFS Debye–Waller factor for the outer coordination shells [7].

In this paper we present original x-ray absorption spectra (XAS) measurements at the As and Ga K edges of GaAs at 77 K and their theoretical calculations. Both EXAFS and XANES (x-ray absorption near-edge structure) regions are considered. The EXAFS signals have been calculated taking into account multiple-scattering contributions through the fast spherical approximation (FSA) approach [8]. This approach has been developed by one of the authors and tested on several compounds with different multiple-scattering contributions (ReO_3, $NaWO_3$, MoO_3, IrO_2) for different core levels (K, L_3), obtaining good agreement with experimental data both in the low- and high-energy ranges [8]. However, the agreement in the low-energy range for some cases can be only qualitative, especially if the multiple-scattering series does not converge fast enough. Therefore, we have used the FSA only for the interpretation of the fine structure at energies greater than $\sim$ 40 eV. The low-energy region (XANES) has been calculated for the first time on both edges using the continued-fraction expansion method developed by Filipponi [9].

The paper is organized as follows. In section 2 the experiment and the procedure for the EXAFS treatment are briefly described. In section 3.1 the method of the EXAFS calculations is shown. Section 3.2 is devoted to the evaluation of the MS contributions and to the analysis of the EXAFS results. The XANES analysis in the framework of the full multiple-scattering approach is discussed in section 4. Section 5 contains the main conclusions.

2. Experimental and data analysis procedure

The sample was prepared as follows. A GaAs monocrystal was finely ground and the powder dispersed in alcohol by an ultrasonic mixer, and then slowly deposited on a polytetrafluoroethylene membrane. The resulting absorption jump was $\Delta\mu x \simeq 1$ at both As and Ga K edges (μ is the absorption coefficient, x is the sample thickness). The XAS on both Ga and As K edges were recorded with synchrotron radiation at the ADONE storage ring (Frascati, Italy) on the PWA BX-2 beamline. The electron energy was 1.5 GeV, the wiggler magnetic field 1.6 T, and the maximum stored current 60 mA. A silicon channel-cut crystal monochromator was used with (220) reflecting faces. The total energy resolution was estimated to be $\Delta E \simeq 1$ eV. The data were recorded with a spacing of 1 eV in the XANES region and 2 eV in the EXAFS region. Two ionization chambers filled with krypton gas were used as detectors. The sample was mounted on a cold finger maintained at 77 K by a liquid nitrogen cryostat.

The data analysis of experimental spectra was carried out following a standard procedure [4, 5]. For each of the two edges (Ga and As) the contribution $\mu_b(E)$ from lower energy edges was approximated according to the Victoreen formula and subtracted from the experimental spectrum. The atomic-like term $\mu_0(E)$ was determined as a sum of cubic polynomials $\mu_p(E)$ and a cubic smoothing-spline $\mu_s(E)$. This procedure allows us to eliminate the contribution of low-frequency signals in the Fourier transform below the first structural peak without any influence on its amplitude.

The EXAFS function was obtained as

$$\chi(E) = \frac{\mu(E) - \mu_b(E) - \mu_0(E)}{\mu_0(E)}. \tag{1}$$

Further analysis was done in k space, where the photoelectron wavevector k is defined as $k = \sqrt{(2m/\hbar^2)(E - E_0)}$ (where m is the electron mass). The energy origin, E_0, was chosen at about 3 eV past the main resonance that corresponds to zero energy in theoretical calculations. The EXAFS signal was Fourier transformed (FT) in the range $k = 2$–$16\,\text{Å}^{-1}$, after weighting by a k factor and convoluting with a Gaussian window.

3. EXAFS analysis

3.1. Calculation of EXAFS signal

The total EXAFS signal including single-, double- and triple-scattering terms has been calculated using the FSA code [8]. In this code the single-scattering term is calculated using the *exact* expression [10], while the double- and triple-scattering terms are calculated using the fast spherical approximation [8]. This is a simplified and fast method for the calculation of the EXAFS function, which can be used even on an IBM PC.

In FSA, as in the simplest multiple-scattering plane-wave approximation (PWA), the atoms involved in the scattering process are considered as *independent modifiers* of the photoelectron wave amplitude, so that the total scattering amplitude function $f_{\text{tot}}(k, \theta)$ is expressed as a product of individual amplitude functions $f_i(k, \theta)$ of all atoms taking part in the scattering of the photoelectron. The main reason for the PWA inaccuracy, i.e. the neglect of the curvature of the photoelectron wave, is eliminated in FSA so that the scattering amplitude function $f(k, \theta)$ is substituted by a distance-dependent function calculated according to the expression [8]

$$f(k, \theta, R) = \frac{1}{k} \sum_{l'} (2l' + 1) t_{l'} P_{l'}(\cos\theta) \sum_{\bar{l}} (2\bar{l} + 1) \left[\begin{pmatrix} l & l' & \bar{l} \\ 0 & 0 & 0 \end{pmatrix} C_{\bar{l}}(kR) \right]^2 \tag{2}$$

where l is the angular momentum of the final state ($l = 1$ for the K edge), θ is the scattering angle, $P_l(x)$ are Legendre polynomials, $C_l(\rho)$ are the polynomial factors introduced by Rehr and co-workers [11] and calculated by a recursion method, the 3×2 matrix is a Wigner ($3j$) symbol, and t_l is the scattering matrix element defined as [10]

$$t_l = \exp(i\delta_l) \sin(\delta_l). \tag{3}$$

The difference between FSA and other approaches (e.g. the separable spherical-wave approximation (SSWA) [12]) is the meaning of the R dependence of the scattering amplitude function: usually R corresponds to the distance between two close-lying atoms along the multiple-scattering path; in FSA it corresponds to *the length of the path from the absorber to the scattering atom*. This leads to the necessity of separate calculations of the double-scattering signals such as $\chi_{A\to B\to C\to A}$ and $\chi_{A\to C\to B\to A}$ so that the total double-scattering contribution from the three-atomic chain is equal to their sum. A comparison of FSA with other existing approaches has been performed for crystalline germanium, which has a crystallographic structure like GaAs: it shows that FSA works better than PWA, gives the same result as SSWA, and differs from the

exact approach mainly in the double-scattering contribution. However, by taking into account the thermal vibrations through the best-fit procedure to experimental data, the MS contribution becomes negligibly small at high energies both for FSA and the exact approaches [13].

The partial phase shifts $\delta_l(k)$ [14] were determined from the radial Schrödinger-like equation for every atom in the cluster by using the MSCALC code developed by Natoli and co-workers [10]. The cluster potential was approximated by spherically averaged *muffin-tin* potentials calculated by a standard Mattheiss procedure [15]. To take into account the covalency of the Ga–As bond the muffin-tin spheres were overlapped by 10%; the so-obtained radii correspond to ones calculated from the Norman criterion [16] and reduced by a factor 0.87 (R_{MT}(Ga) = 1.3211 Å and R_{MT}(As) = 1.3719 Å). The final state of the absorbing atom (Ga or As) was considered as fully relaxed, with a hole localized at the 1s level.

The complex Hedin–Lundqvist (HL) potential, based on the density functional formalism within the single-plasmon pole approximation, was used as the exchange and correlation potential (ECP) [17]. It allowed us to take into account inelastic losses of the photoelectron in extrinsic channels on plasmon excitations, and thus to correct the amplitude of calculated spectra for estimating the electron mean-free path (MFP). In figure 1 the MFP $\lambda(k)$ calculated from the imaginary part of the HL potential are shown (as a function of the photoelectron wavevector). The sharp increase of the MFP at lower energies means that below the plasmon energy λ tends to infinity. It is also possible to define the effective mean-free path, λ, which takes into account the core-hole level width Γ of the K excited state:

$$\lambda = \frac{\hbar}{\Gamma_t(E)}\left(\frac{2E}{m}\right)^{1/2} \qquad \Gamma_t = \Gamma_h + \frac{\hbar}{\lambda(E)}\left(\frac{2E}{m}\right)^{1/2}. \tag{4}$$

The Γ_h values were taken from [18]: Γ_h = 2.13 eV for the Ga K edge and Γ_h = 2.57 eV for the As K edge. As shown in figure 1, the core-hole level width reduces the MFP and is most important at low energies. In figure 1 we also report the mean-free path values obtained by Stern and co-workers [2] from EXAFS measurements on both Ga and As K edges in GaAs (figure 16(*a*) of [2]). The central circle at each temperature corresponds to the most likely value, the lower and higher circles reflect the influence of the uncertainty in determining the Debye–Waller factors. The agreement between our calculated values and the experimental ones of [2] is only partial; possible causes of the discrepancy are: (i) the rather involved procedure used to extract the mean-free path from experimental data, and (ii) the non-negligible degree of uncertainty in the values of core-level widths Γ_h available in the literature [18, 19] and used in (4). However, the difference in core-level widths has a weak influence on the shape of the EXAFS spectra for both edges.

3.2. Evaluation of multiple-scattering contributions

To estimate the influence of multiple-scattering effects on the EXAFS in GaAs, some calculations were performed for three model systems using the FSA.

(i) A cluster As_1–Ga_0–As_2 consisting of three atoms with R(Ga–As) = 2.4481 Å and the value of the As–$\widehat{Ga}$–As angle varying from 90°–180°.

(ii) A cluster Ga_0–As_1–Ga_2 consisting of three atoms with R(Ga–Ga) = 3.9977 Å and the value of the Ga–$\widehat{As}$–Ga angle varying from 90°–180°.

(iii) A five-shells cluster with the *exact* GaAs structure.

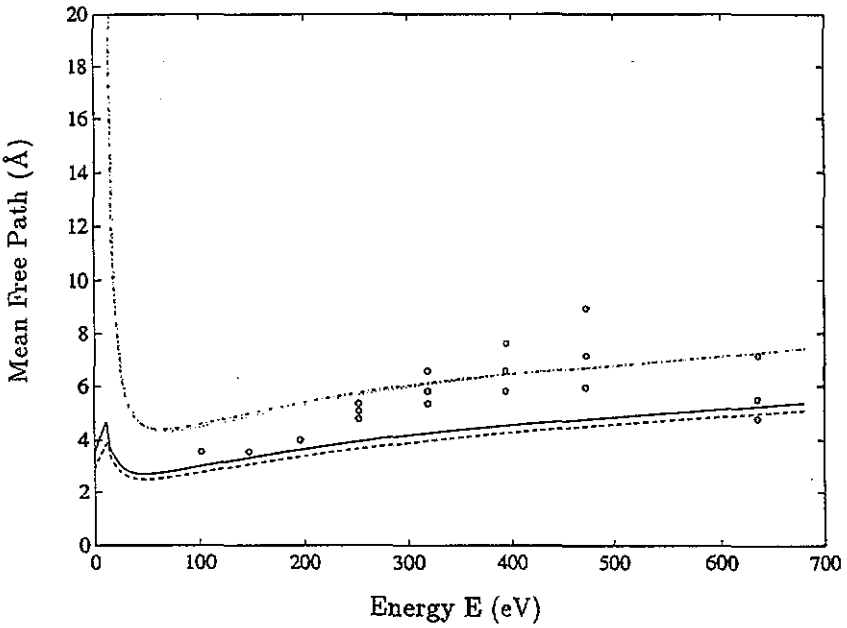

Figure 1. Photoelectron mean-free path $\lambda(E)$ as a function of energy calculated from the imaginary part of the Hedin–Lundqvist potential for GaAs (chain curve: K edge Ga, dotted curve: K edge As). Full and broken curves correspond to effective mean-free paths $\lambda_{\text{eff}}(E)$ taking into account the core-hole level width $\Gamma_h = 2.13$ and 2.57 eV for gallium and arsenic K edges, respectively. Circles indicate the mean-free path from [2].

The index 0 indicates the central atom (absorber), and the indices 1 and 2 correspond to two different neighbouring atoms. Because of the finite photoelectron mean-free path and the effects of thermal vibrations, only multiple-scattering events within the first and second shells are expected to give a significant contribution to the total signal.

To estimate the multiple-scattering contribution as a function of bonding angle, the two artificial models, (i) and (ii), were considered first. It is known that atomic chains with nearly linear structure give the main contribution to the EXAFS signal among all other MS paths. The two chosen models allowed us to evaluate the range of bonding angles in which the MS correction is important. The MS paths used in the calculations are shown in table 1. They concern the first coordination shell of the central atom in model (i), and the second shell in model (ii).

In the case of the As_1–Ga_0–As_2 model, the distance Ga–As was fixed to be 2.4481 Å and the value of the angle As–$\widehat{Ga}$–As was varied from 90°–180°. It was found that the MS signal contributes in R space at the location of the third shell of the real crystal structure, and its amplitude strongly depends on the bonding angle (see figure 2(a)). One can distinguish two angular intervals: from 90°–120° the MS contribution is practically negligible, while above 120° it grows and reaches its highest value for the linear As_1–Ga_0–As_2 chain. In the real crystal structure of GaAs this angle is 109.5°, and all three atomic chains in the first shell are equivalent: so one can conclude that the MS contributions generated within the first coordination shell in GaAs are negligible.

For the Ga_0–As_1–Ga_2 model the distance Ga–Ga was fixed to be 3.9977 Å and the angle Ga–$\widehat{As}$–Ga was varied from 90°–180°. In this case the MS signal contributes in R space at the location of the second shell in the real crystal structure. Its amplitude

Table 1. Multiple-scattering paths used in calculations for the three-atom clusters As_1–Ga_0–As_2 and Ga_0–As_1–Ga_2.

Cluster	MS order	Path	Degeneracy
As_1–Ga_0–As_2	Single scattering	0–1–0	4
	Double scattering	0–1–2–0	12
	Triple scattering	0–1–0–1–0	4
		0–1–0–2–0	12
Ga_0–As_1–Ga_2	Single scattering	0–2–0	12
	Double scattering	0–1–2–0	12
		0–2–1–0	12
	Triple scattering	0–1–2–1–0	12
		0–1–0–2–0	12
		0–2–0–1–0	12

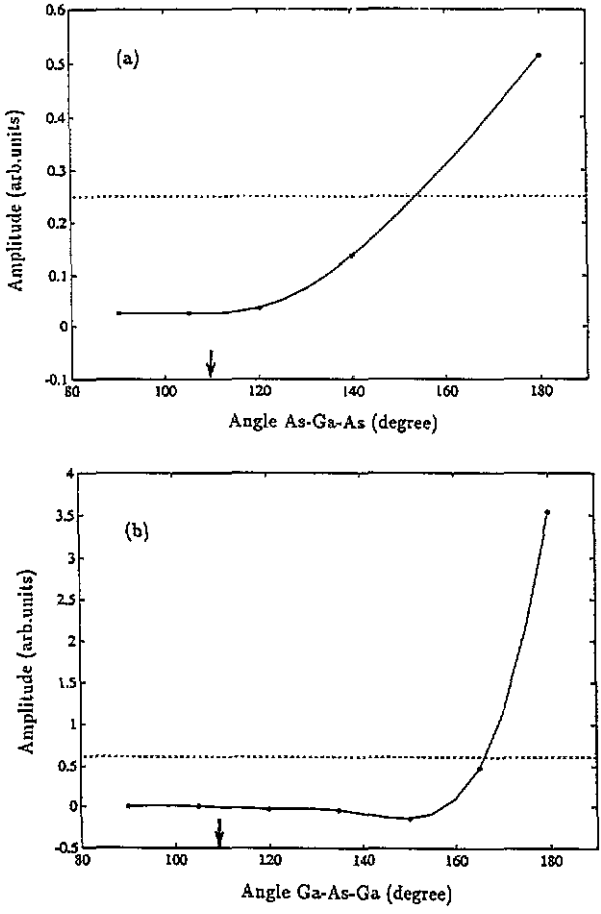

Figure 2. (*a*) Dependence of multiple-scattering contribution from the bonding angle As–$\widehat{Ga}$–As in the As_1–Ga_0–As_2 cluster in comparison with the single-scattering signal from the third shell in the real crystal (horizontal line). The arrow indicates the actual value of the angle in GaAs crystal. (*b*) Dependence of multiple-scattering contribution from bonding angle Ga–$\widehat{As}$–Ga in the Ga_0–As_1–Ga_2 cluster in comparison with the single-scattering signal from the second shell in the real crystal (horizontal line). The arrow indicates the actual value of the angle in GaAs crystal.

strongly depends on the bonding angle as for model (i) (see figure 2(*b*)), although in a more complicated way: below 135° the MS contribution is negligible, from 135°–155° it slightly modifies the total EXAFS, and only above 155° does it lead to a considerable increase of the EXAFS amplitude. The Ga–$\widehat{As}$–Ga angle in the GaAs crystal is again 109.5° because Ga and As atoms are in equivalent positions, so one can conclude that the MS contributions from the second shell are negligible too.

Table 2. Crystallographic data for GaAs (gallium is the central atom) from [20].

Atomic pair	Coordination number	Distance, Å
$Ga–As_1$	4	2.4481
$Ga–As_2$	12	3.9977
$Ga–As_3$	12	4.6877
$Ga–As_4$	6	5.6537
$Ga–As_5$	12	6.1609

Table 3. Multiple-scattering paths used in calculations for the five-shells cluster with exact GaAs structure. Atom numbers 1 to 5 identify coordination shells; atom 6 is an atom in the first coordination shell, different from atom 1. The best-fit Debye–Waller σ^2 values for each path refer to Ga K edge (without brackets) and As K edge (within brackets).

MS order	Path	Degeneracy	σ^2, Å^2 ($\pm$0.0005)
Single scattering	0–1–0	4	0.0017 (0.0021)
	0–2–0	12	0.0027 (0.0023)
	0–3–0	12	0.0031 (0.0035)
	0–4–0	6	0.0040 (0.0040)
	0–5–0	12	0.0045 (0.0045)
Double scattering	0–1–6–0	12	0.0029 (0.0035)
	0–1–2–0	12	0.0031 (0.0032)
	0–2–1–0	12	0.0031 (0.0032)
Triple scattering	0–1–0–1–0	4	0.0035 (0.0042)
	0–1–0–6–0	12	0.0035 (0.0042)
	0–1–2–1–0	12	0.0035 (0.0042)
	0–1–0–2–0	12	0.0045 (0.0044)
	0–2–0–1–0	12	0.0045 (0.0044)

A more refined analysis for both Ga and As K edges has been done for a cluster with exact GaAs structure [20] up to the fifth coordination shell (table 2). The paths included in the calculations and their degeneracies are shown in table 3. To obtain the best agreement with experimental data, the amplitude of the calculated curves for both edges was multiplied by a factor $S_0^2=0.8$, which describes the intrinsic losses of the photoelectron. The Debye–Waller (DW) factors of single-scattering paths were set as free parameters, and used to express the DW factors of multiple-scattering paths by the method proposed in [4]:

$$\sigma^2_{a_1,a_2,\ldots a_n} = \frac{1}{2}\sum_{i=1}^{n-1}\sigma^2_{a_i,a_i+1} \qquad a_n \equiv a_1 \tag{5}$$

where a_i indicates the ith atom along the multiple-scattering path. This approach is a very simplified way of estimating the effect of thermal vibrations in the MS signals; a more precise analysis could be done according to the theory of Benfatto and co-workers [21]. The results of the best-fit procedure are shown in table 3. The discrepancies between the DW factors obtained for the same bonds from the Ga and As edges can be accounted for by the uncertainty in the fitting procedure and by the intrinsic limitations of (5).

The calculated EXAFS curves and their FT are compared with experimental data in figures 3 and 4. The agreement between calculated and experimental curves is very good. The separate contributions from single, double and triple scatterings to the

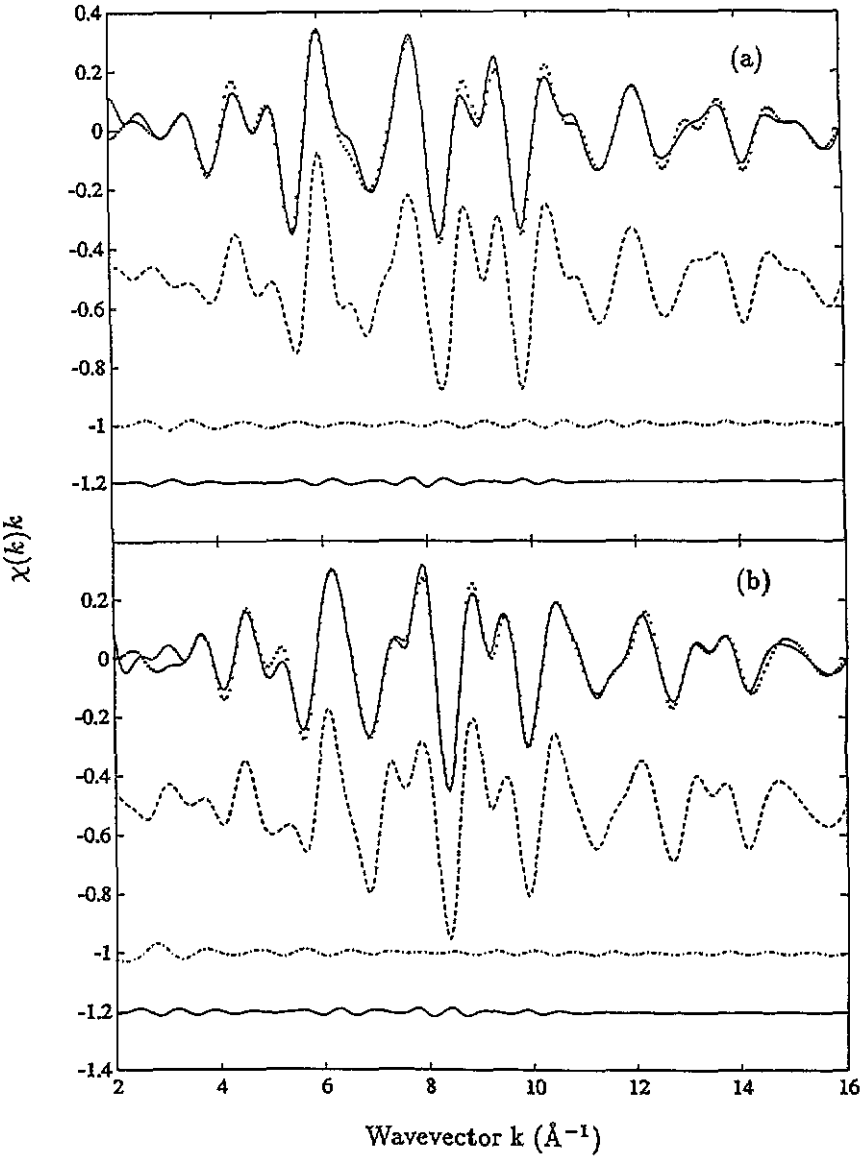

Figure 3. Contributions from single (broken curve), double (chain curve) and triple (lower full curve) scattering paths for the five-shells cluster to the total spectrum (full curve) for Ga (*a*) and As (*b*) K edges. The 77 K experimental spectra are shown by dots for comparison with the total calculated signals.

total spectrum are shown in figures 3(*a*) and (*b*). For wavevector values greater than 3–3.5 Å^{-1} the MS contribution is everywhere less than 5% of the SS signal. This is due to the small amplitude of the true MS signal and to thermal vibrations which further decrease the signal. Only for lower energies is it more important, growing to 50% at 2 Å^{-1}. This behaviour is mainly due to a peculiarity of the backscattering amplitude of Ga and As, which has a minimum at 3 Å^{-1}. Our results show that the EXAFS in GaAs can be analysed above 3 Å^{-1} in terms of the single-scattering approximation

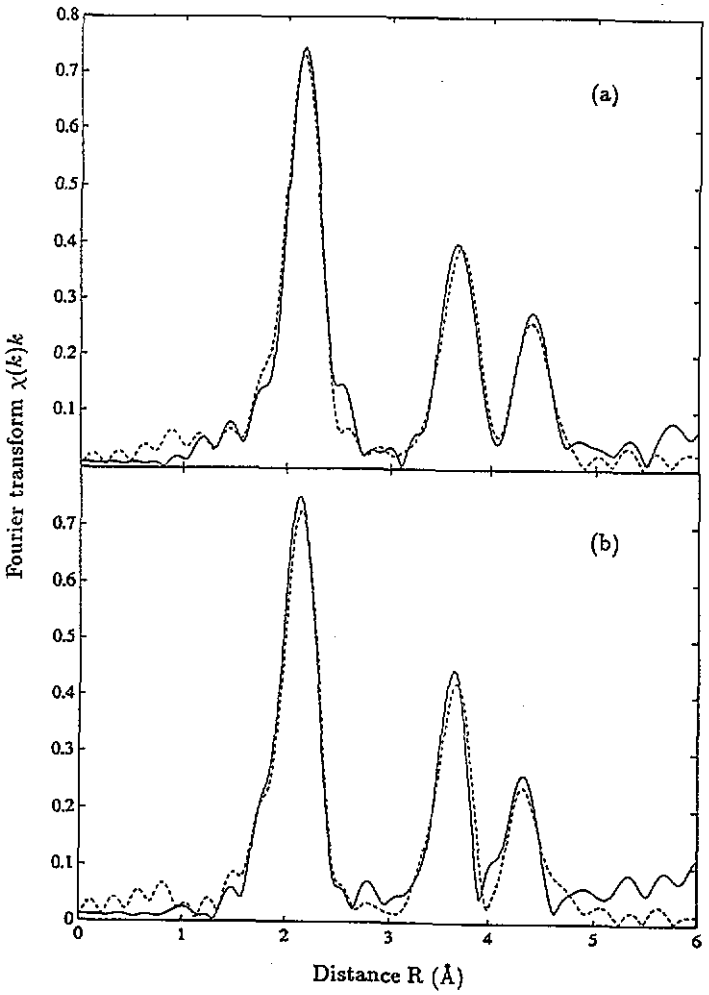

Figure 4. Fourier transforms of the EXAFS $\chi(k)k$ spectra for Ga (*a*) and As (*b*) K edges in GaAs. Full curves are the 77 K experimental spectra. Broken curves are the calculations for the five-shells cluster.

without significant loss of accuracy. This confirms the conclusions of [2].

4. XANES analysis

Gallium and arsenic atoms are located at equivalent crystallographic positions in GaAs, and they are very close in the periodic table. This explains the similarity of their EXAFS. Their XANES, however, are quite different (figure 5). The first peak is due to a direct transition to the bound state: it is slightly more prominent for Ga than for As; the second peak, which is well separated for Ga, is mixed with the first one for As. To explain this interesting fact, an analysis of the near-edge structure has been done for the first time on both the Ga and As K edges. We have used an interpretation scheme in which the transitions to bound states and the scattering processes are singled out and separately

analysed. The contribution from the latter ones was calculated using the *full multiple-scattering approach*, based on the *continued-fraction expansion* method developed by Filipponi [9]. In fact, FSA cannot give a precise description of the fine structure in the XANES range due to the slow convergence of the MS series in this region and, in addition, to the limits of the approximation.

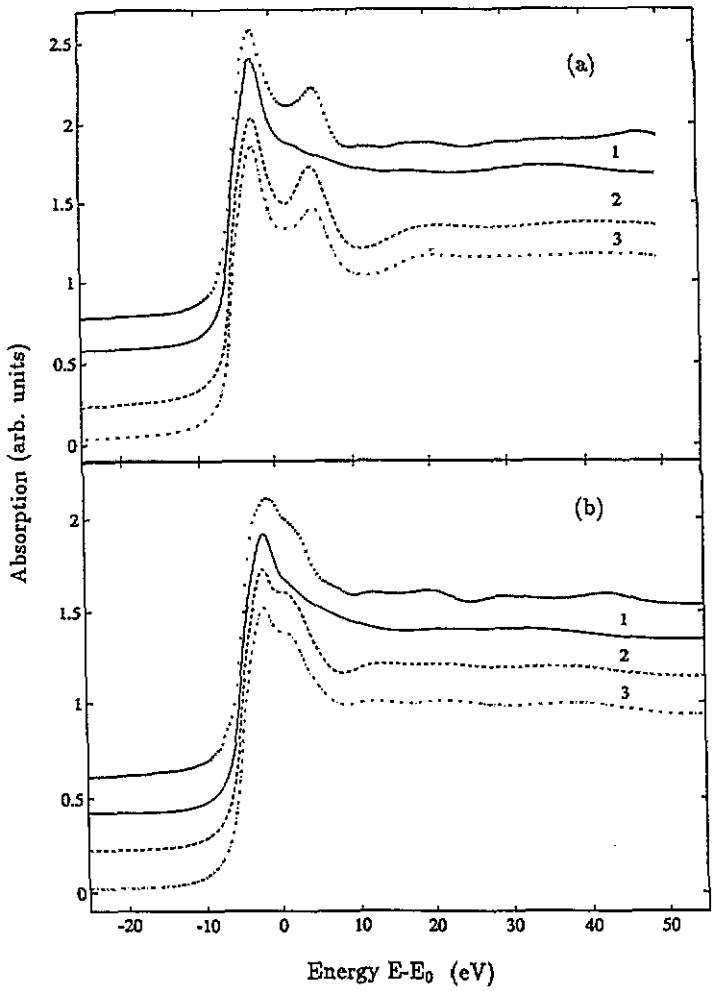

Figure 5. XANES for the Ga (*a*) and As (*b*) K edges in GaAs. The experimental spectrum (dots) is compared with calculated spectra for clusters of the different sizes: first (full curve), second (broken curve) and third (chain curve) coordination shells around the absorbing atom.

The total cross section $\sigma_{tot}(E)$ was calculated by the following expression:

$$\sigma_{tot}(E) = \sigma_{res}(E) + \sigma_0(E)(1 + \chi(E)). \tag{6}$$

Here $\sigma_{res}(E)$ is the contribution from the bound-to-bound $1s \rightarrow 4p$ transition: it can be approximated by a Lorentzian curve, whose height and width are chosen by a best fit to the first peak; $\sigma_0(E)$ is the contribution of transitions from the 1s level of the

absorbing atom to the continuum of the unoccupied free-electron-like states in the absence of surrounding atoms, and is defined as [22]

$$\sigma_0(E) = \tfrac{1}{2} + (1/\pi)\tan^{-1}[2(E - E_0)/\Delta] \tag{7}$$

where E_0 is the energy of the continuum threshold, which corresponds to the energy origin used in EXAFS calculations, and Δ defines the slope of the $\sigma_0(E)$ in the edge region; $\chi(E)$ is the fine structure due to photoelectron scatterings on atoms of the cluster and was calculated using the continued-fraction expansion method [9]. In figure 5(a) and (b) the experimental spectra are compared with those calculated for clusters of different sizes (first, second and third coordination shells around the absorbing atom). The fine structure past ~ 30 eV above the first main feature has already been calculated by a multiple-scattering approach to EXAFS; we therefore concentrate our attention on lower energies.

As a result of the fitting procedure, we have ascertained that both Lorentzians for the Ga and As edges had the same amplitude, while their widths were different ($\Gamma_{Ga} = 2.6$ eV, $\Gamma_{As} = 3.1$ eV). These widths coincide, within the fitting uncertainty, with the corresponding Δ parameters in (7) obtained by the same best-fit procedure. They are also in good agreement with total broadenings $\Gamma_{tot} = \Gamma_{cl} + \frac{1}{2}\Gamma_{exp}$ [23], where Γ_{cl} are the Ga and As K edges core-level widths reported in [18] and $\Gamma_{exp} \simeq 1$ eV is the experimental resolution.

Coming now to the $\chi(E)$ term in (6), the near-edge structure beyond the first peak cannot be satisfactorily reproduced by taking into account only one coordination shell. The addition of the second coordination shell leads to a sufficiently good agreement with experimental data. In particular it gives us an explanation for the second feature, which is located at 10376 eV in the Ga spectra and at 11870 eV in the As spectra. It can be interpreted as a scattering resonance in the second coordination shell of the excited atom (Ga or As), and its shift to lower energies for the arsenic K edge is due to the different phase shifts of the photoelectron wave in the case of the Ga–Ga and As–As pairs. The addition of the third coordination shell does not change appreciably the calculated curve. Only minor modifications of the cross section amplitude are introduced. A better agreement with experimental data could be obtained by increasing the number of coordination shells involved in the calculation, as shown by Sainctavit and co-workers [24] for ZnS, which has the same crystallographic structure of GaAs.

The influence on the calculations of other factors, such as overlap of MT spheres and lifetime broadening, was also tested. It was found that changes of the MT spheres overlap in the range 5–20% lead to a slight smoothing of the calculated spectrum without significantly affecting the main shape. The broadening influences only the sharpness of the second feature.

5. Summary

In this paper a theoretical interpretation of the x-ray absorption fine structure in the framework of the multiple-scattering (MS) approach for the GaAs crystal on both the Ga and As edges is presented. The calculated spectra are in good agreement with experimental data in both the XANES and EXAFS regions. It has been shown that the MS contribution to the EXAFS spectra is negligible for wavevector values greater than $3\,\text{Å}^{-1}$ due to the small amplitude of the MS signal itself and, in addition, due to the

presence of the thermal damping. Therefore the single-scattering analysis can be used without significant loss of accuracy in that region. The XANES calculations done for the first time allowed us to explain the difference between the near-edge structures of the Ga and As edges. This is due to the change in core-level widths and phase shifts of the photoelectron wave under scattering from the Ga or As atoms located in the second coordination sphere.

Acknowledgments

The authors are thankful to C R Natoli and co-workers for the use of the MSCALC code. They wish also to thank A Filipponi for the possibility of using his XANES code for cross section calculations, and J Purans for helpful discussions. They are thankful to E Burattini and technical staff of the PWA laboratory for support during experiments. AK wish to thank Professor G Dalba and his collaborators for hospitality and financial support during his stay at the University of Trento. DD wishes to thank the 'ICTP programme for training and research in Italian Laboratories, Trieste, Italy' for partial support during this work.

References

[1] Engström O (ed) 1986 *Proc. 18th Int. Conf. on Phys. of Semiconductors* vols 1& 2 (Singapore: World Scientific)
Christou A and Rupprecht H S (eds) 1987 *Proc. 14th Int. Symp. GaAs and Related Compounds* vol 91 (Bristol: Adam Hilger)
[2] Stern E A, Bunker B A and Heald S M 1980 *Phys. Rev.* B **21** 5521–39
[3] Hung N V 1989 *Exp. Tech. Phys.* **37** 203–12
[4] Teo B K 1986 *EXAFS: Basic Principles and Data Analysis* (Berlin: Springer)
[5] Sayers D E and Bunker B A 1988 *X-Ray Absorption: Principles, Applications, Techniques of EXAFS, SEXAFS and XANES* ed D C Koningsberger and R Prins (New York: Wiley)
[6] Hasnain S S (ed) 1991 *Proc. 6th Int. Conf. on x-ray Absorption Fine Structure* (Chichester: Ellis Horwood)
Dalba G, Fornasini P, Rocca F and Mobilio S 1990 *Phys. Rev.* B **41** 9668–75
[7] Dalba G, Diop D, Fornasini P and Rocca F 1992 *Japan. J. Appl. Phys.* to be published
[8] Kuzmin A and Purans J 1993 *J. Phys.: Condens. Matter* **5** 267–82
Kuzmin A and Purans J 1992 *Japan. J. Appl. Phys.* to be published
[9] Filipponi A 1991 *J. Phys.: Condens. Matter* **3** 6489–507
[10] Ruiz-López M F, Loops M, Goulon J, Benfatto M and Natoli C R 1988 *Chem. Phys.* **121** 419–37
Natoli C R and Benfatto M 1986 *J. Physique Coll.* **47** C-8 11–23
[11] Rehr J J, Albers R C, Natoli C R and Stern E A 1986 *Phys. Rev.* B **34** 4350–3
[12] Houser B, Ingalls R and Rehr J J 1992 *Phys. Rev.* B **45** 8097–9
[13] Kuzmin A (unpublished results)
[14] Schiff L I 1955 *Quantum Mechanics* (New York: McGraw-Hill)
[15] Mattheiss L F 1964 *Phys. Rev.* A **134** 970–3
[16] Norman J G 1974 *Mol. Phys.* **81** 1191
[17] Hedin L and Lundqvist B I 1971 *J. Phys. C: Solid State Phys.* **4** 2064–83
[18] Keski-Rahkonen O and Krause M O 1974 *At. Data Nucl. Data Tables* **14** 140
[19] Sevier K D 1972 *Low Energy Electron Spectrometry* (New York: Wiley)
[20] Wyckoff R W G 1963 *Crystal Structures* vol 1 (New York: Wiley)
[21] Benfatto M, Natoli C R and Filipponi A 1989 *Phys. Rev.* B **40** 9626–35
[22] Richtmeyer E K, Barnas S W and Ramberg E 1934 *Phys. Rev.* B **46** 843
[23] Kisiel A, Dalba G, Fornasini P, Podgórny M, Oleszkiewicz J, Rocca F and Burattini E 1989 *Phys. Rev.* B **39** 7895–904
[24] Sainctavit Ph, Petiau J, Benfatto M and Natoli C R 1990 *Proc. 2nd Eur. Conf. on Progress in X-Ray Synchrotron Radiation Research* ed A Balerna *et al* (Bologna: SIF)